Experimental band structure of ordered Cu overlayers on Ag(001)

N. G. Stoffel,* S. D. Kevan, and N. V. Smith
AT&T Bell Laboratories, Murray Hill, New Jersey 07974
(Received 4 February 1985)

We present an extensive systematic study of the electronic structure and epitaxial growth of ordered Cu films on clean Ag(001) surfaces. Angle-resolved photoemission with synchrotron radiation was used to map the two-dimensional band dispersions of monolayers and multilayers of Cu using several photon energies. Band symmetries were determined from polarization selection rules. At room temperature we observe pseudomorphic growth of Cu films for film thicknesses up to three atomic layers. Although our epitaxial results are very similar to those reported recently, we find a Cu $3d$-band width more than twice as large. This discrepancy is attributed to their failure to observe the lowest Cu $3d$ bands. These bands are difficult to observe since they overlap intense Ag $4d$ emission at many photon energies. The use of polarized synchrotron radiation allowed us to measure the energy of the true d-band minimum. The Cu $3d$-band width (3.15 eV) is virtually identical to that of bulk Cu, but the band center is about 0.25 eV lower. The band topology agrees well with calculations for supported and unsupported Cu monolayers, but theory tends to underestimate the $3d$-band width.

I. INTRODUCTION

The investigation of the electronic structure of molecular and atomic adsorbates on d-band metal surfaces has long been a major preoccupation of surface science. Only recently has attention shifted toward the problem of d-band-metal overlayers on other metals. These metal-overlayer systems possess a much more complicated valence electronic structure than do the more common adsorbates. The preparation of clean, well-characterized metal overlayers also entails more experimental difficulties.

The recent application of slab-calculation techniques[1–6] to the determination of several metal-overlayer electronic structures coincides with a growing experimental interest[6–10] in this area. These efforts have demonstrated that monolayer films of metals can exhibit new magnetic, chemical, and electronic properties or alter those properties of the substrate metal surface. These effects are thought to be intimately related to changes in d-band width, position, and occupancy which are, in turn, affected by charge transfer, strained bonds, rehybridization, and changes in coordination number occurring at the surface and interface. The accurate experimental determination of the electronic structure of overlayers of d-band metals provides a valuable test of current theoretical understanding of these interdependent phenomena.

We have performed extensive angle-resolved photoelectron spectroscopy (ARPES) measurements of the band structure for the ordered overlayer system, Cu/Ag(001). This system presents several practical advantages for such a study. It has filled overlayer d bands, which makes possible a complete ARPES band mapping. The bulk and surface electronic structures of Ag and Cu have been well established by much previous ARPES work.[11,12] The Cu $3d$ bands are found to lie almost entirely above the Ag $4d$ bands, which simplifies interpretation of the photoemission spectra. The initial room-temperature growth of Cu has been reported to be layer by layer,[8,13] and the overlayer unit cell is (1×1) with Cu atoms almost certainly continuing the face-centered-cubic Ag lattice with suitable relaxations of the interlayer spacings. This structure can be handled efficiently in the slab calculations, and retains the high symmetry of the Ag(001) surface. Therefore, simple parity selection rules[14] can be applied to the initial states along the $\bar{\Delta}$ and $\bar{\Sigma}$ symmetry axes. Finally, the inertness of these noble-metal surfaces reduces the effects of surface contamination on our results.

Our experimental methods are discussed in the succeeding section, followed by a presentation and analysis of some typical ARPES spectra in Sec. III. We present the measured Cu overlayer band structure in Sec. IV along with a discussion of current theoretical results.

II. EXPERIMENTAL TECHNIQUES

The substrate employed in this experiment was a 1-cm-diam Ag single crystal which had been cut and polished to expose a (001) plane. Several hours of neon-ion bombardment to remove surface damage, followed by annealing to 1000 K, resulted in a sharp (1×1) low-energy electron diffraction (LEED) pattern. Cu was evaporated onto the room-temperature Ag crystal from an electron-bombardment-heated tantalum crucible within a liquid-nitrogen-cooled shroud. The pressure rose to $(1-1.5)\times10^{-9}$ Torr during evaporations. The evaporation rate was monitored by a quartz-crystal microbalance to determine the Cu coverage in terms of a substrate monolayer equivalent ($1\ \mathrm{ML}\equiv5.98\times10^{14}$ atoms cm^{-2}). The calibration of the microbalance was checked by measuring the Cu-to-Ag Auger intensity ratio as a function of nominal Cu thickness after successive evaporations. Breaks in the slope of the Auger ratio are expected in a layer-by-layer growth mode.[7] Discontinuities were

observed at monolayer and bilayer coverages, but higher coverages resulted in a smooth increase in the Cu-to-Ag intensity ratio. Above about 4 ML this increase was distinctly slower than would be expected for uniform Cu overlayer formation, indicating the onset of three-dimensional island growth. Sharp commensurate (1×1) LEED patterns were observed from the Cu monolayers, with a slight increase in the diffuse background up to 3-ML coverage. However, an additional 3 ML of Cu led to a dramatic decrease in long-range order with LEED beams becoming barely discernible. An analogous result is seen in the ARPES spectra, where the sharpness and angular dependence of the Cu-induced features decreases abruptly between 3- and 6-ML coverage. Our epitaxial results are essentially the same as those reported by Smith *et al.*[15] for the Cu/Ag(001) system. Those authors report pseudomorphic growth through at least 2 ML.

The experiments were performed with a toroidal-grating monochromator[16] at the National Synchrotron Light Source. ARPES spectra were collected with a spherical deflector analyzer on a two-axis goniometer.[17] The acceptance angle was 1.5° or less and the overall resolution was better than 200 meV. The determination of the electronic structure of the Cu overlayers involved the acquisition of hundreds of ARPES spectra. Five parameters were varied independently in this experiment. Polar and azimuthal emission angles were varied to map the band dispersions $E(\mathbf{k}_{\|})$, while photon energy was changed to verify their two-dimensional nature. The evolution of the electronic structure was observed as Cu coverage was increased in increments. Finally, photon polarization was changed to obtain band symmetries.

Auger measurements indicated a substantially higher reactivity for CO on the Cu overlayers than on the clean Ag(001) surface. Therefore, a clean Ag(001) substrate was prepared prior to the deposition of each Cu overlayer, and a complete series of ~100 ARPES spectra was completed within 15 h for each surface. At an operating pressure of 2×10^{-10} Torr changes in the Cu/Ag spectra were not observed until after about 60 h of exposure to the residual gases.

III. ARPES SPECTRA AND DISCUSSION

We will present only a small portion of the ARPES spectra which illustrates the techniques used to distinguish and identify those features which are associated with the two-dimensional (2D) Cu overlayer electronic structure. A series of spectra for 1-ML coverage of Cu on Ag(001) is presented in Fig. 1. These spectra, extending to $\theta=60°$ off-normal along the [010] azimuth, probe states of even symmetry along the $\bar{\Sigma}$ line in the surface Brillouin zone (SBZ) which is illustrated in Fig. 2.

Since the $4d$ bands of Ag are found entirely in the region below -3.75-eV binding energy, the spectral features at 2 to 3.5 eV below the Fermi level E_F are easily identified as Cu $3d$ bands. These contributions are indicated by tick marks in Fig. 1 along with a series of shoulders near -5.4 eV. The latter weak features do in fact originate from the Cu $3d$ band as will become evident below in the discussion of Fig. 3. The $\bar{M}$ point of the Ag SBZ corresponds to a wave vector parallel to the surface $\mathbf{k}_{\|}$ of magnitude $|\mathbf{k}_{\|}|=1.53$ Å^{-1}. The peaks denoted by tick marks near -5.4 eV in Fig. 1 roughly span the range of wave vectors $1.2\leq|\mathbf{k}_{\|}|\leq1.8$ Å^{-1}. Here we have employed the usual kinematic formula to determine $|\mathbf{k}_{\|}|$,

$$|\mathbf{k}_{\|}|=0.5123(\text{Å}^{-1})(E_k)^{1/2}\sin\theta\,, \tag{1}$$

where E_k is the kinetic energy (in electron volts) at which the feature is observed. This formulation assumes conservation of $\mathbf{k}_{\|}$ during the photoemission process. The shoulder at -5.4 eV for 1 ML Cu develops into a distinct peak at higher Cu coverages as seen in Fig. 3. We em-

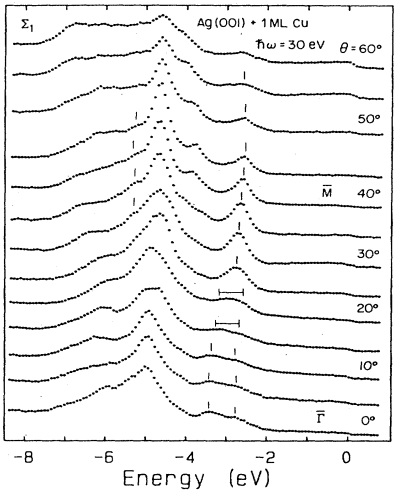

FIG. 1. Series of ARPES spectra taken at 5° increments of polar angle θ along the $\bar{\Sigma}$ azimuth for 1 ML Cu on Ag(001). The photon energy is 30 eV and the polarization vector is in the plane of detection, so states of Σ_1 symmetry are favored. Three bands of features (indicated by the tick marks), which we attribute to Cu $3d$ states, are seen to disperse in energy as θ is varied. The Cu $3d$ origin of the features is established by comparison with data from clean Ag and from Ag with 2–6 monolayers of Cu coverage as explained in the text. Emission at $\theta=40°$ originates near the $\bar{M}$ symmetry point.

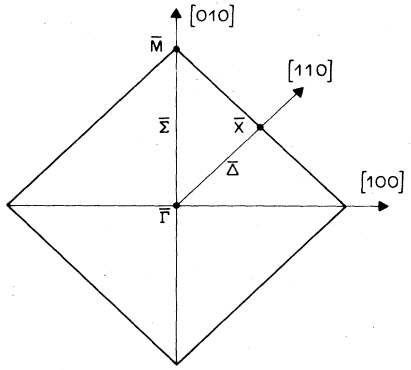

FIG. 2. First Brillouin zone of the (001) surface.

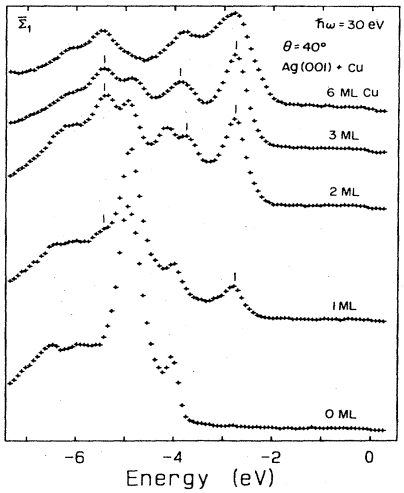

FIG. 3. Comparison of ARPES spectra taken for 0—6 monolayers of Cu on Ag(001) at angle corresponding closely to $\bar{M}$. Two additional features are induced by adding a Cu monolayer to the clean Ag surface. A third Cu peak is evident at higher Cu coverages. Polarization selection rules select states of Σ_1 symmetry in the collection geometry employed for these spectra. The spectra were normalized to have equal areas under the curves.

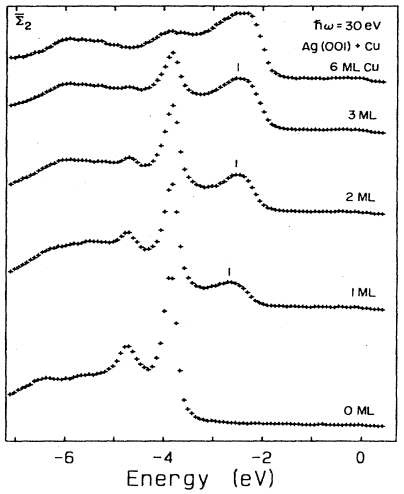

FIG. 4. Data taken under identical conditions to Fig. 3, except that states of Σ_2 symmetry are favored in this collection geometry. Both Ag and Cu bands display clear symmetry selection rules.

phasize the importance of such comparisons of Cu monolayer spectra with those for multilayers and clean Ag in our identification of the lower Cu $3d$ states. In several instances the 1 ML Cu spectra display weak features in the energy range of the Ag $4d$ band which are absent in the clean Ag(001) spectra. These features are only identified as Cu $3d$-band states if similar features also appear with equal or greater intensity in the 2- and 3-ML Cu spectra. If not, we assume they are due to Ag $4d$—derived states for which the photoemission intensity and/or angle is changed by the addition of a Cu overlayer. The latter effect might arise from increased scattering due to the higher density of defects on the Cu covered surface than on the clean, annealed Ag surface. We shall not discuss here the interesting alternative explanation that these features are intrinsic interface states, since there seems to be no conclusive way to distinguish these from the aforementioned spurious effects.

For 2—6-ML coverages the highest-energy peak in Fig. 3 gains intensity while another peak develops at -3.5 eV. All three Cu $3d$ bands identified in Fig. 3 at the $\bar{M}$ point have even parity with respect to the $\bar{\Sigma}$ mirror plane of the surface. This becomes more obvious upon a comparison of Figs. 3 and 4 which differ only in the orientation of the polarization vector of the incident photons; parallel to the mirror plane in Fig. 3 and almost perpendicular to it in Fig. 4. Since the photoelectrons are detected in this mirror plane, even and odd states will be emphasized, respectively, according to the selection rules outlined by Hermanson.[14] Strong selection-rule effects are apparent in both the bulk Ag and overlayer Cu d bands. In particular, the -3.5- and -5.4-eV features due to Cu clearly display even symmetry while states of both symmetries appear near -2.5 eV.

Similar selection rules hold in the $\bar{\Delta}$ mirror plane. Even states with $\mathbf{k}_{\parallel}$ just short of the $\bar{X}$ point are shown in Fig. 5. Note that a strong peak develops with Cu coverage at -5.4 eV, while two barely resolved features appear at -2.9 and -3.4 eV. A comparison with odd polarization spectra (not shown) demonstrates the even symmetry of the two more tightly bound Cu-derived states. In addition, the even sp bands of both Cu and Ag are evident in this figure near -1.5 and -0.4 eV, respectively. Both sp bands have dispersions of about 0.5 eV per degree of polar angle. The slight variation in their energy with coverage

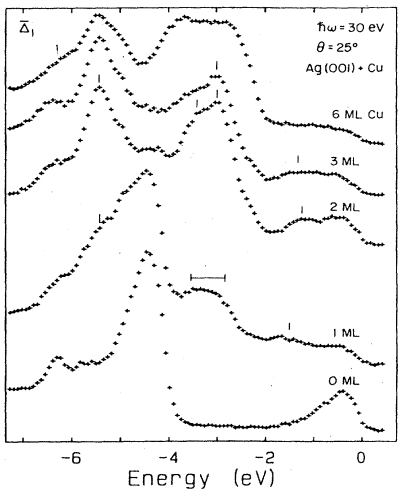

FIG. 5. Data taken under the same conditions of Fig. 3, except that the azimuth and angle correspond to a point almost all of the way along $\bar{\Delta}$ to $\bar{X}$. States of Δ_1 symmetry are seen in this geometry, including Ag and Cu sp bands at low binding energy.

is possibly due to small sample misalignments. Both *sp* bands disperse above E_F at $\bar{X}$ for spectra obtained using 30-eV photon energy. Note that the Cu *sp* band does not become more intense with increasing Cu coverage as do the *d* bands. The widths of the peaks in Figs. 3—5 increase markedly between 3- and 6-ML coverage. As mentioned earlier, this correlates with the loss of long-range order as seen by LEED and indicates the limits of pseudomorphic growth of Cu on Ag(001).

IV. TWO-DIMENSIONAL BAND STRUCTURE

We have identified those features in our ARPES data which correspond to transitions from the Cu overlayer using the criteria described in the preceding section, and mapped the two-dimensional band structure using Eq. (1). The results of this mapping along the $\bar{\Sigma}$ and $\bar{\Delta}$ azimuths are presented in Fig. 6 for 1-ML Cu coverage. Accurate binding energies were obtained using an algorithm to fit the ARPES spectra with Lorentzian-shaped peaks. The position, width, and area of each peak were allowed to vary freely in the fitting procedure. In some instances where the photoemission intensity is low or where two bands approach one another, the algorithm cannot resolve individual peaks, and so error bars spanning the probable peak positions are presented.

The data of Fig. 6 are derived only from the spectra of Cu monolayers. Data from Cu bilayers and trilayers are presented in Fig. 7. The differences in peak positions for Cu monolayers and multilayers are usually less than 0.2 eV, suggesting that we are measuring nearly the same 2D band structure in either case. Some additional band structure is observed for the multilayer Cu films. The 2D nature of the band structure is supported by the fact that Figs. 6 and 7 contain data taken at photon energies of 30 and 40 eV. These data overlay one another, indicating that the Cu band structure is independent of $\mathbf{k}_\perp$, the perpendicular wave-vector component of the photoemission final state. In contrast, the bulk Ag bands show a strong $\mathbf{k}_\perp$ dependence between 30 and 40 eV as expected due to their three-dimensional nature. In a further test, $\mathbf{k}_\perp$ independence was also confirmed for Cu-derived bands of Δ_1 symmetry over the larger range of $\mathbf{k}_\perp$ afforded by the use of photon energies between 15 and 40 eV.

The curves drawn through the data of Figs. 6 and 7 have the same qualitative topology and the same symmetry as the calculated band structures of supported[1,3,5,18] and unsupported[19–21] Cu monolayers. In most cases the calculated bands would have to be widened and placed at a greater binding energy in order to coincide with our experimental results. The resulting Cu 3*d*-band width and binding energy are much closer to those of bulk Cu than to those calculated for the unsupported monolayers (which are 2.5—2.7 eV wide and cross or nearly cross the Fermi energy).[19–21] The extremes of the bulk *d* bands of Cu have been reported by several groups.[11] They extend from −2.0 eV (X_5) to −5.2 eV (X_1). The monolayer *d* bands we observe extend from −2.25 eV ($\bar{M}_3$) to −5.4 eV ($\bar{M}_4$). Thus they are more tightly bound and, somewhat surprisingly, as wide as the bulk Cu 3*d* bands.

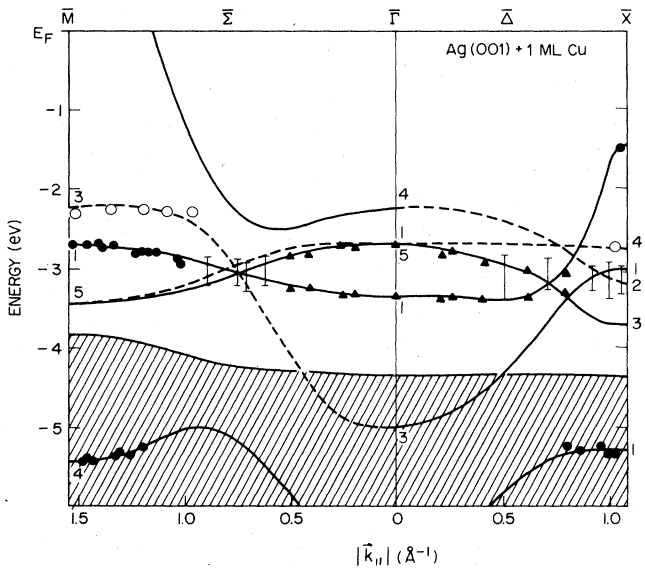

FIG. 6. Band mapping of the 2D electronic structure of the Cu monolayer which has been reduced to the first Brillouin zone. Features displaying clear Δ_1 or Σ_1 symmetry are indicated by solid circles while open circles represent Δ_2 or Σ_2 states. The remaining features are plotted as triangles or, in the case of unresolved peaks, as error bars spanning the probable peak positions. Data taken at 30- and 40-eV photon energies are included. Bands are drawn through the points in qualitative agreement with theory as discussed in the text. Bands with Σ_2 or Δ_2 symmetry are indicated by dashed lines. The shaded area indicates the projection of the Ag 4*d* bulk band structure.

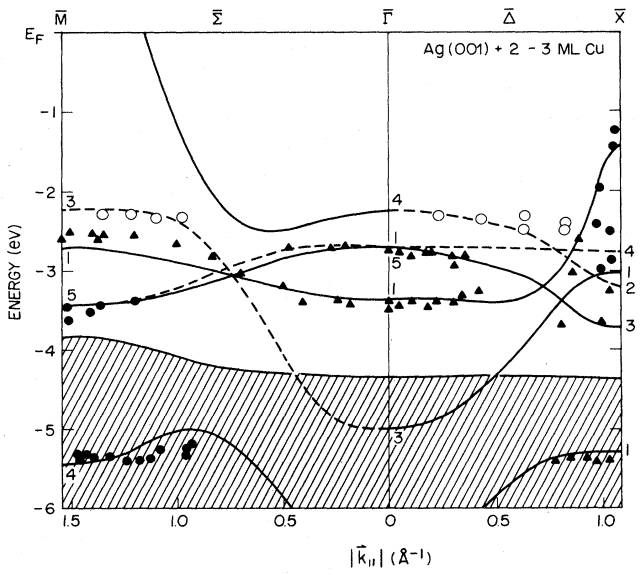

FIG. 7. Band mapping of two- and three-monolayer Cu data. The curves through the data are identical to those of Fig. 6. Only well-resolved features are included for clarity.

Our observation of low-lying (−5.4 eV) Cu-induced features was unanticipated in previous photoemission studies[15,22] where it was generally concluded that the Cu $3d$ bands are quite narrow and lie entirely above the Ag $4d$ band. Earlier works report a d-band width of less than 1.5 eV while we find a width of 3.15 eV. The discrepancy arises entirely from the neglect of photoemission features overlapping the Ag $4d$ bands. We note that we find almost identical peak positions at $\bar{\Gamma}$ and $\bar{M}$ for the upper Cu $3d$ bands as reported in Ref. 15. The limited number of spectra we have gathered at 20 eV contain strong contributions from Ag $4d$ bands which would interfere with the identification of the $\bar{M}_4$ and $\bar{X}_1$ emission at −5.4 eV. This interference is greatly reduced for 30- and 40-eV photon energies. The use of polarized light, reducing the number of Ag $4d$ peaks in the ARPES spectra, also facilitates identification of the Cu $3d$ features. Finally, the $\bar{X}_1$ and $\bar{M}_4$ emission becomes quite strong at higher coverages of Cu, but is fairly weak in the monolayer ARPES spectra. Thus, it would be difficult to identify correctly without a systematic study at several coverages such as we have performed.

Calculations of the density of states for a copper monolayer and for an Ag-supported monolayer are reported by Bisi and Calandra.[1] In contrast to the free-standing monolayer results,[19–21] which report very shallow d bands, they place the d bands 1 eV below the bulk Cu $3d$ position. They ascribe most of this lowering to the 13% linear expansion of the Ag-supported Cu monolayer. The measured lowering is only 0.25 eV. We note that the density of states for Cu/Ni(001) calculated by Tersoff and Falicov[3] comes as close to agreement with our results as any calculation of which we are aware, both in bandwidth and position. Since there is negligible lattice strain in the Cu/Ni(001) system, we question whether the lattice expansion is a major factor in determining band position and width. We are also forced to reject the contention that bandwidth simply decreases inversely as the fifth power of lattice constants of the monolayer. This dependence, proposed originally by Heine,[23] is used by Smith *et al.* to explain the small apparent width of the d bands they report. However, it was derived in the context of the three-dimensional bulk lattice expansion, and its application to the Cu/Ag(001) system is not straightforward. If there is a tendency toward band narrowing because of the lattice expansion (or the reduced coordination of the surface Cu atoms), it is clearly offset by other factors. These might include the effects of d-d and s-d interaction between Cu and Ag or of the bcc-like local geometry of the strained Cu(001) overlayer. Theoretical and experimental studies of other (001) epitaxial monolayers might help to elucidate these factors.

In a study of the complementary system, Ag/Cu(001), Tobin *et al.*[9] find only 2D band dispersions for 1- or 2-ML Ag coverages. Three-dimensional band structure begins to become evident at 4-ML coverages where some peaks in the ARPES spectra display a photon-energy dependence. Likewise, we observe only 2D behavior up to the limit of pseudomorphic growth, which occurs at about 3-ML Cu.

V. CONCLUSIONS

We have measured the band structure of Cu for ordered thin films along the two mirror planes of the Ag(001) surface. Our results agree qualitatively with the calculated two-dimensional band structures for a free-standing Cu monolayer. The 3.15-eV width we observe for the Cu $3d$ bands is essentially identical to that reported for bulk Cu (3.2 eV), but contrasts sharply with the 1.5-eV bandwidth reported in an earlier ARPES experiment. The monolayer bands are more tightly bound than the bulk bands by about 0.25 eV. The band dispersions of Cu seem to be described reasonably well in terms of $\mathbf{k}_{\parallel}$ alone for <3-ML-thick Cu films. Pseudomorphic films of greater thickness apparently cannot be formed on Ag(001) at room temperature.

ACKNOWLEDGMENTS

This work was conducted at the National Synchrotron Light Source (Upton, N.Y.), which is supported by the U.S. Department of Energy (Division of Materials Sciences and Division of Chemical Sciences).

*Permanent address: Bell Communications Research, Murray Hill, NJ 07974.

[1]O. Bisi and C. Calandra, Surf. Sci. **67**, 416 (1977).
[2]Ding-Sheng Wang, A. J. Freeman, and H. Krakauer, Phys. Rev. B **24**, 1126 (1981).
[3]J. Tersoff and L. M. Falicov, Phys. Rev. B **25**, 2959 (1982).
[4]D. D. Loly and J. B. Pendry, J. Phys. C **16**, 423 (1983).
[5]Hong Huang, Xue-Yuan Zhu, and J. Hermanson, Phys. Rev. B **29**, 2270 (1984); **29**, 3009 (1984).
[6]M. El-Batanouny, D. R. Hamann, S. R. Chubb, and J. W. Davenport, Phys. Rev. B **27**, 2575 (1983).
[7]G. C. Smith, H. A. Padmore, and C. Norris, Surf. Sci. **119**, L287 (1982).
[8]C. Binns, C. Norris, G. C. Smith, H. A. Padmore, and M. G. Barthes-Labrousse, Surf. Sci. **126**, 258 (1983).
[9]J. G. Tobin, S. W. Robey, L. E. Klebanoff, and D. A. Shirley, Phys. Rev. B **28**, 6169 (1983).
[10]R. Miranda, D. Chandresris, and J. Lecante, Surf. Sci. **130**, 269 (1983).
[11]For a summary of results on Cu, see R. Courths, V. Bachelier, B. Cord, and S. Hüfner, Solid State Commun. **40**, 1059 (1981), and references therein.
[12]P. S. Wehner, R. S. Williams, S. D. Kevan, D. Denley, and D. A. Shirley, Phys. Rev. B **19**, 6169 (1979).
[13]L. A. Bruce and H. Jaeger, Philos. Mag. **36**, 1331 (1977).
[14]J. Hermanson, Solid State Comm. **22**, 9 (1977).
[15]G. C. Smith, C. Norris, and C. Binns, J. Phys. C **17**, 4389 (1984).

[16]P. Thiry, P. A. Bennett, S. D. Kevan, W. A. Royer, E. E. Chaban, J. E. Rowe, and N. V. Smith, Nucl. Instrum. Methods **222**, 85 (1984).
[17]S. D. Kevan, Rev. Sci. Instrum. **54**, 1441 (1983).
[18]Xue-Yuan Zhu, Hong Huang, and J. Hermanson, Phys. Rev. B **29**, 3009 (1984).
[19]G. S. Painter, Phys. Rev. B **17**, 3848 (1978).
[20]C. S. Wang and A. J. Freeman, Phys. Rev. B **18**, 1714 (1978).
[21]J. R. Smith, J. G. Gay, and F. J. Arlinghaus, Phys. Rev. B **21**, 2201 (1980).
[22]D. E. Eastman and W. D. Grobman, Phys. Rev. Lett. **30**, 177 (1973).
[23]V. Heine, Phys. Rev. **153**, 673 (1967).